

# Precise Determination of QED Contribution to Lepton $g-2$

T. Aoyama

KMI, Nagoya University

based on the work carried out in collaboration with  
T. Kinoshita, M. Nio, M. Hayakawa, N. Watanabe, K. Asano

KMI International Symposium 2013  
on “Quest for the Origin of Particles and the Universe”  
December 11–13, 2013, Nagoya

- Electrons and Muons have magnetic moment along their spins, given by

$$\vec{\mu} = g \frac{e\hbar}{2m} \vec{s}$$

It is known that  $g$ -factor deviates from Dirac's value ( $g = 2$ ), and it is called **Anomalous magnetic moment**

$$a_\ell \equiv (g - 2)/2$$

- Historically it is found in Zeeman splitting of Galium atom which showed that electron's  $g$ -factor is about 0.1% larger than the prediction of Dirac eq.:

$$a_e(\text{exp}) = 0.001\ 15\ (4)$$

Kusch, Foley, PR72, 1256 (1947)

- Schwinger's calculation leads to:

$$a_e(\text{theory}) = 0.001\ 161\ \dots$$

Schwinger, PR73, 416L (1948); PR75, 898 (1949)

This was one of the early triumphs of renormalized theory of QED.

- Latest measurement by Harvard group by spin precession of a single electron in cylindrical Penning trap:

$$a_e(\text{exp}) = 0.001\ 159\ 652\ 180\ 73\ (28) \quad [0.24\text{ppb}]$$

Hanneke, Fogwell, Gabrielse, PRL 100, 120801 (2008)

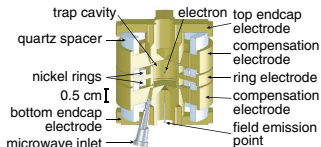


FIG. 2 (color). Cylindrical Penning trap cavity used to confine a single electron and inhibit spontaneous emission.

- Latest theoretical prediction within Standard Model:

$$a_e(\text{theory}) = 0.001\ 159\ 652\ 181\ 78\ (77) \quad [0.67\text{ppb}]$$

TA, Hayakawa, Kinoshita, Nio, PRL 109, 111807 (2012)

- Experiment and theory are in good agreement with each other:

$$a_e(\text{exp}) - a_e(\text{theory}) = -1.05\ (82) \times 10^{-12}$$

This indicates that QED (Standard Model) is valid even at this precision.

- Contributions to lepton  $g-2$  within the context of the standard model consist of:

$$a_\ell = a_\ell(\text{QED}) + a_\ell(\text{Hadronic}) + a_\ell(\text{Weak})$$

and their proportion is:

	electron	muon
QED (mass-independent)	999999.996 ppm	994623 ppm
QED (mass-dependent)	0.0023 ppm	5313 ppm
Hadronic	0.0014 ppm	$\sim 60$ ppm
Weak	0.00003 ppm	1 ppm

(ppm =  $10^{-6}$ )

$$a_e(\text{QED}) = A_1 + \underbrace{A_2(m_e/m_\mu) + A_2(m_e/m_\tau) + A_3(m_e/m_\mu, m_e/m_\tau)}_{\text{mass-dependent contribution}}$$

- Therefore electron  $g-2$  is explained almost entirely by QED interaction between electron and photons. It has provided the most stringent test of QED.
- Muon  $g-2$  is more sensitive to high energy physics, and thus a window to new physics beyond the standard model. The precise determination of QED contribution provides a baseline.

- QED corrections are evaluated by perturbation theory:

$$a_e(\text{QED}) = A^{(2)} \left( \frac{\alpha}{\pi} \right) + A^{(4)} \left( \frac{\alpha}{\pi} \right)^2 + A^{(6)} \left( \frac{\alpha}{\pi} \right)^3 + A^{(8)} \left( \frac{\alpha}{\pi} \right)^4 + \dots$$

- Up to which order of the QED perturbation theory do we need, to meet the precision of the measurements?

Considering that

$$\begin{aligned} \left( \frac{\alpha}{\pi} \right)^4 &\simeq 29.1 \times 10^{-12}, \\ \left( \frac{\alpha}{\pi} \right)^5 &\simeq 0.067 \times 10^{-12}, \end{aligned}$$

and the experimental uncertainty

$$\delta a_e(\text{exp}) = 0.28 \times 10^{-12},$$

evaluation of 10th-order term  $A^{(10)}$  has to be considered seriously.

- Up to 6th order terms are known analytically.  
8th and 10th order terms are evaluated by numerical means.

		year	# diagram
$A_1^{(2)} = 0.5$	Schwinger	1948	1
$A_1^{(4)} = -0.328\ 478 \dots$	Sommerfield, Petermann	1957	7
$A_1^{(6)} = 1.181\ 241 \dots$	Laporta & Remiddi (analytic)	1996	72
	Kinoshita (numerical)	1995	
$A_1^{(8)} = -1.910\ 6\ (20)$	Kinoshita & Nio	2005	891
	TA, Hayakawa, Kinoshita, Nio	2007,2012	
$A_1^{(10)} = 9.16\ (58)$	TA, Hayakawa, Kinoshita, Nio	2012	12,672

- To compare the theoretical prediction with the experiment, the value of the fine structure constant  $\alpha$  is needed which is determined by an independent method.
- The best value of such  $\alpha$  has been obtained recently from the measurement of  $h/m_{\text{Rb}}$  combined with Rydberg constant and  $m_{\text{Rb}}/m_e$ :

$$\alpha^{-1}(\text{Rb}) = 137.035\,999\,037\,(91)$$

Bouchendir *et al.*, PRL 106, 080801 (2011)

- With this  $\alpha$ , the theoretical prediction of  $a_e$  becomes:

$$a_e(\text{theory}) = 1\,159\,652\,181.82\,(0.06)(0.02)(0.78) \times 10^{-12}$$

uncertainty comes from 8th order term, 10th order term, and uncertainty of  $\alpha(\text{Rb})$ .

- From the measurement and the theory of electron  $g-2$ , the value of fine-structure constant can be determined.

Experimental value  $\rightarrow a_e =$

Theoretical calculations  $\rightarrow$

$$a_e = A^{(2)} \left(\frac{\alpha}{\pi}\right) + A^{(4)} \left(\frac{\alpha}{\pi}\right)^2 + A^{(6)} \left(\frac{\alpha}{\pi}\right)^3 + A^{(8)} \left(\frac{\alpha}{\pi}\right)^4 + A^{(10)} \left(\frac{\alpha}{\pi}\right)^5 + \dots$$

+ (small contributions)

$\alpha^4$ $\alpha^5$ had+ew exp (7) (5) (2) (33)
--

- Newly obtained value of fine-structure constant is:

$$\alpha^{-1}(a_e) = 137.035\,999\,173\,(35) \quad [0.25\text{ppb}]$$

c.f.  $\alpha^{-1}(\text{Rb}) = 137.035\,999\,037\,(91) \quad [0.66\text{ppb}]$

$$\alpha^{-1}(\text{Cs}) = 137.036\,000\,00\,(110) \quad [8.0\text{ppb}]$$

Bouchendira *et al.*, PRL 106, 080801 (2011)

Wicht, *et al.*, Phys. Scr. T102, 82 (2002)

Gerginov, *et al.*, PRA 73, 032504 (2006)

- Latest world average of the measured  $a_\mu$ :

$$a_\mu[\text{exp}] = 116\,592\,089\,(63) \times 10^{-11} \quad [0.5\text{ppm}]$$

Bennett, et al., Phys. Rev. D73 (2006) 072003,  
 Roberts, Chinese Phys. C 34, 741 (2010).

- Summary of theoretical values: (in units of  $10^{-11}$ )

QED 2nd	116 140 973.318	( 0.077)
4th	413 217.6291	( 0.0090)
6th	30 141.902 48	( 0.00041)
8th	381.008	( 0.019)
10th	5.0938	( 0.0080)
<hr/>		
$a_\mu(\text{QED})$	116 584 718.951	( 0.080)
<hr/>		
Hadronic		
LO v.p.	6 949.1	(42.7)
NLO v.p.	98.4	( 0.7)
l-by-l	116	(40)
Weak	154	( 2)
<hr/>		
$a_\mu(\text{SM})$	116 591 840	(59)

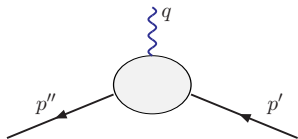
- Discrepancy between experiment and theory is:

$$a_\mu(\text{exp}) - a_\mu(\text{SM}) = 249\,(87) \times 10^{-11}$$

- Magnetic property of lepton can be studied through examining its scattering by a static magnetic field.

The amplitude can be represented as:

$$e\bar{u}(p'') \left[ \gamma^\mu F_1(q^2) + \frac{i}{2m} \sigma^{\mu\nu} q_\nu F_2(q^2) \right] u(p') A_\mu^e(\vec{q})$$



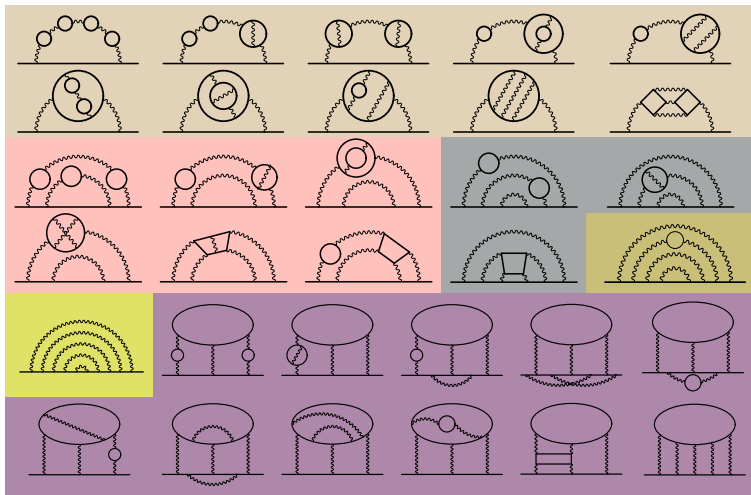
- The anomalous magnetic moment is the static limit of the magnetic form factor  $F_2(q^2)$ :

$$a_\ell = F_2(0) = Z_2 M, \quad M = \lim_{q^2 \rightarrow 0} \text{Tr}(P_\nu(p, q)\Gamma^\nu)$$

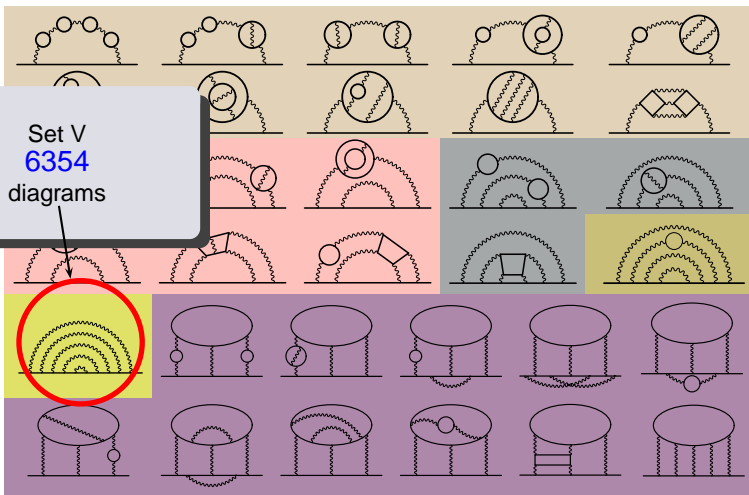
where  $\Gamma^\nu$  is the proper vertex function with the external lepton on the mass shell, and  $P_\nu(p, q)$  is the magnetic projection operator.

# 10th-order correction

- Number of diagrams contributing to 10th order  $A_1^{(10)}$  is 12,672.
- they are classified into 32 gauge-invariant sets shown as follows:



- the largest and most difficult one is Set V consists of 6354 diagrams that have no lepton loops.

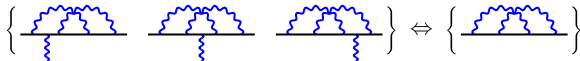


- Our strategy:
  - Evaluate diagrams separately by numerical means.
  - Amplitude of each diagram must be a finite calculable value.
  - Renormalize theory **exactly** to highest order needed, and in a form suitable for evaluation on a computer.
- Procedure:
  - Step 1. Find distinct set of Feynman diagrams.
  - Step 2. Construct **amplitude** in terms of Feynman parametric integral.
  - Step 3. Construct subtraction terms of **UV divergence**.
    - *K*-operation
  - Step 4. Construct subtraction terms of **IR divergence**.
    - *I*-subtraction of logarithmic IR divergences.
    - *R*-subtraction of residual mass-renormalization.
  - Step 5. Carry out **residual renormalization** to achieve standard on-shell renormalization.

- Combined uncertainty of contributions from  $N$  diagrams grows roughly as  $\sqrt{N}$ . Thus it is important to reduce the number of independent integrals.
- A set of vertex diagrams  $\Lambda$  obtained by inserting an external vertex into each lepton line of self-energy diagram  $\Sigma$  can be related by Ward-Takahashi identity.

$$\Lambda^\nu(p, q) \simeq -q_\mu \left. \frac{\partial \Lambda^\mu(p, q)}{\partial q_\nu} \right|_{q \rightarrow 0} - \frac{\partial \Sigma(p)}{\partial p_\nu}.$$

e.g. 4th-order case:

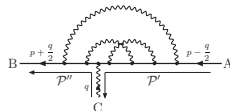
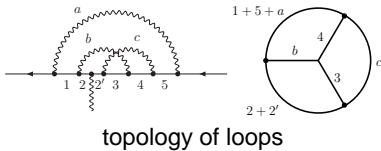


- For Set V diagrams, the number of independent integrals goes from **6354** to **706** by WT sum, further reduced by time-reversal symmetry to **389**.

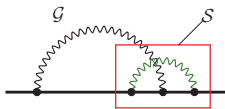
- Amplitude is given by an integral over loop momenta according to Feynman-Dyson rule.
- It is converted into Feynman parametric integral over  $\{z_i\}$ . Momentum integration is carried out analytically, and it yields

$$M_G^{(2n)} = \left(-\frac{1}{4}\right)^n \Gamma(n-1) \int (dz)_G \left[ \frac{F_0}{U^2 V^{n-1}} + \frac{F_1}{U^3 V^{n-2}} + \dots \right]$$

- Integrand is expressed by a rational function of terms called *building blocks*,  $B_{ij}$ ,  $A_j$ ,  $U$ ,  $C_{ij}$  and  $V$ .
- Building blocks are given by functions of  $\{z_i\}$ , reflecting the topology of diagram, flow of momenta, etc.



- UV divergence occurs when loop momenta in a subdiagram go to infinity. It corresponds to the region of Feynman parameter space  $z_i \sim \mathcal{O}(\epsilon)$  for  $i \in S$ .



- In order to carry out subtraction numerically, the singularities are cancelled point-by-point on Feynman parameter space.

$$M_G - L_S M_{G/S} \longrightarrow \int (dz)_G \left[ m_G - \mathbb{K}_S m_G \right]$$

- IR divergence of each diagram may occur in a particular region of Feynman parameter space that corresponds to some photons goes soft. This singularity is also subtracted point-by-point way.
- Subtraction terms are so constructed that they can be factorized into (divergent part of) renormalization constant and lower-order magnetic part.

$$\int (dz)_G \left[ \mathbb{K}_S m_G \right] = L_S^{\text{UV}} M_{G/S}$$

This property is crucial for the **residual renormalization** step.

- This formulation can be generalized to higher order diagrams.
- Finite amplitude  $\Delta M_G$  free from both UV and IR divergences is obtained by Feynman-parameter integral as:

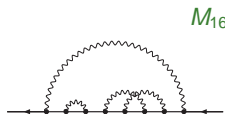
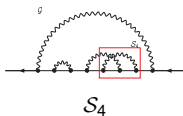
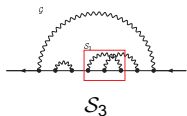
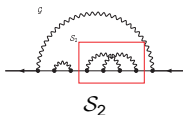
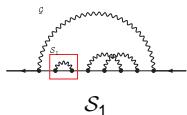
$$\Delta M_G = \int (dz) \left[ F_G \quad \leftarrow \text{unrenormalized amplitude} \right. \\ \left. + \sum_f \prod_{S \in f} (-\mathbb{K}_S) F_G \quad \leftarrow \text{UV subtraction terms} \right. \\ \left. + \sum_{\tilde{f}} (-\mathbb{I}_{S_i}) \cdots (-\mathbb{R}_{S_j}) \cdots F_G \right] \quad \leftarrow \text{IR subtraction terms}$$

*f*: Zimmermann's forests:  
combinations of UV divergent subdiagrams.

$\tilde{f}$ : *annotated* forests:  
combinations of self-energy subdiagrams  
with distinction of *I*/*R*-subtractions.

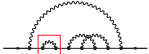
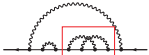
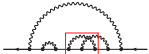
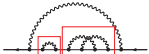
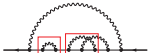
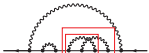
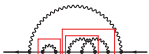
- Identification of divergent parts is diagram-based, and suitable for automated treatment.

- Consider an 8th order case,  $M_{16}$ , which have two self-energy subdiagrams ( $S_1, S_2$ ), and two vertex subdiagrams ( $S_3, S_4$ ).



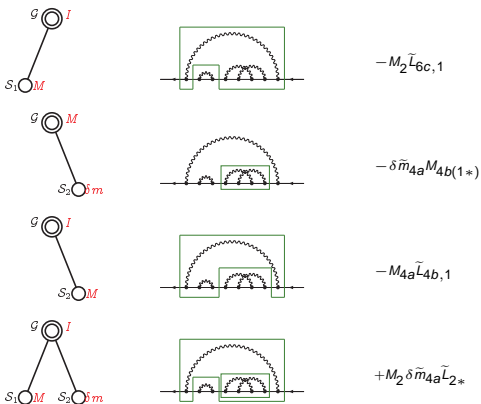
- Relations between subdiagrams are:
  - $S_1$  and  $S_2, S_3, S_4$  are *independent*.
  - $S_2$  *contains*  $S_3, S_4$ .
  - $S_3$  and  $S_4$  are *cross-overlapping*.

- According to Zimmermann's forest formula, UV divergent parts and corresponding subtraction terms are identified as:

$\{S_1\}$		$-\delta\hat{m}_2 M_{6c(1^*)} - \hat{B}_2 M_{6c}$
$\{S_2\}$		$-\delta\hat{m}_{4a} M_{4b(1^*)} - \hat{B}_{4a} M_{4b}$
$\{S_3\}, \{S_4\}$		$-\hat{L}_2 M_{6a} \quad (\times 2)$
$\{S_1, S_2\}$		$+\delta\hat{m}_2 \delta\hat{m}_{4a} M_{2^{**}} + \delta\hat{m}_2 \hat{B}_{4a} M_{2^*} + \hat{B}_2 \delta\hat{m}_{4a} M_{2^*} + \hat{B}_2 \hat{B}_{4a} M_2$
$\{S_1, S_3\}, \{S_1, S_4\}$		$+\delta\hat{m}_2 \hat{L}_2 M_{4b(1^*)} + \hat{B}_2 \hat{L}_2 M_{4b} \quad (\times 2)$
$\{S_2, S_3\}, \{S_2, S_4\}$		$+\hat{L}_2 \delta\hat{m}_2 M_{4b(1^*)} + \hat{L}_2 \hat{B}_2 M_{4b} \quad (\times 2)$
$\{S_1, S_2, S_3\},$ $\{S_1, S_2, S_4\}$		$-\delta\hat{m}_2 \hat{L}_2 \delta\hat{m}_2 M_{2^{**}} - \delta\hat{m}_2 \hat{L}_2 \hat{B}_2 M_{2^*} - \hat{B}_2 \hat{L}_2 \delta\hat{m}_2 M_{2^*} - \hat{B}_2 \hat{L}_2 \hat{B}_2 M_2 \quad (\times 2)$

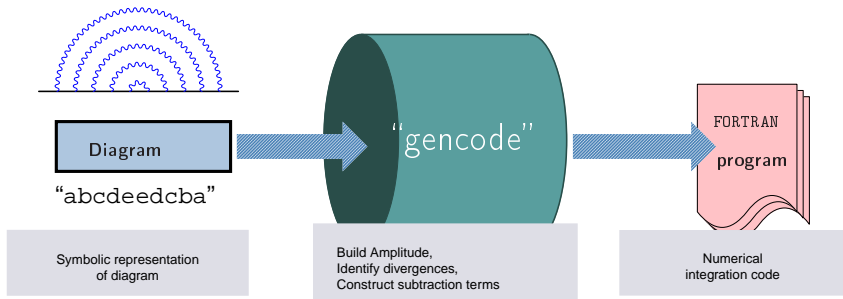
# "Annotated forests" for IR subtraction

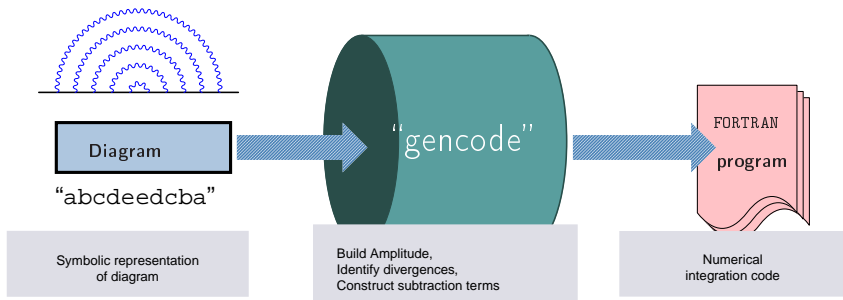
- IR subtraction terms are identified by combination of self-energy type subdiagrams with distinction of  $I$ - or  $R$ -subtraction operation as:



- UV subdivergent terms



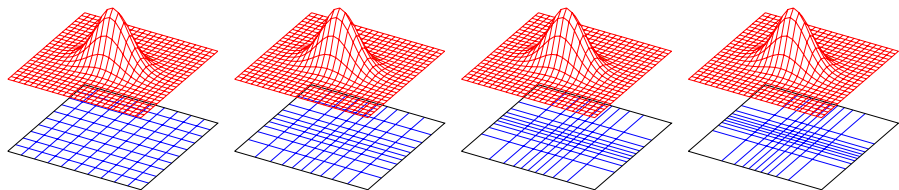




- 10–20 min./diagram for code generation on ordinary PC.
- Program size amounts to  $\mathcal{O}(10^5)$  FORTRAN lines per diagram.
- “gencode” is tailored so that it can process any order of diagrams. This enables us to check the validity of the code generator by lower order diagrams.

TA, Hayakawa, Kinoshita, Nio, Nucl. Phys. B 740, 138 (2006)  
TA, Hayakawa, Kinoshita, Nio, Nucl. Phys. B 796, 184 (2008)

- The amplitude is expressed as a multi-dimensional integral. ( $D = 14 - 1$  for 10th-order diagrams)
- The integrand is a huge rational function. The size of integrand is  $\mathcal{O}(10^5)$  lines of FORTRAN code per diagram.
- Numerical integration is performed by an adaptive-iterative Monte-Carlo method, VEGAS. (Lepage, 1978)
- Integral over  $s$ -dimensional region  $I^s = [0, 1]^s$  is evaluated from  $N$  independent samples of a random variable that is distributed according to  $\rho(x)$  within  $I^s$ .



VEGAS: adaptive grid adjustment during iterations

- Divergences are dealt with subtractive scheme point-by-point in the parameter space. Severe digit-deficiency problem may occur.
- IEEE754 double-precision floating point format:

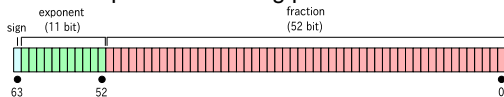


figure taken from Wikipedia

resolution is  $2^{-53}$  (16–17 digits).

- A remedy is to employ extended precision arithmetic (quadruple, etc).  
e.g. express a floating-point value  $a$  by a set of double-precision data  $a_0, a_1, \dots$  as:

$$a = a_0 + \epsilon a_1 + \epsilon^2 a_2 + \dots, \quad \epsilon = 2^{-53}$$

Arithmetics over  $a$  are translated to those over  $a_i$ 's, by passing rounding-off residues to lower order components based on Knuth and Dekker algorithm.

We use “double-double” and “quadruple-double” of `qd` library  
Bailey, Hida, Li. c.f. <http://crd.lbl.gov/~dhbailey/mpdist/>

- Numerical calculations are mainly conducted on supercomputers in RIKEN.
  - RIKEN Super Combined Cluster (RSCC)  
Apr. 2005 – Jun. 2009
  - RIKEN Integrated Cluster of Clusters (RICC)  
Oct. 2009 –
- Several other facilities are used e.g. workstations in Nagoya University, and KMI  $\varphi$  cluster computing system.



- 2012 updates on QED contribution to lepton  $g-2$ :
  - The complete 10th order term that consists of 12,672 vertex Feynman diagrams is evaluated.
  - The numerical precision of 8th order contribution is improved.
  - The improved value of the fine structure constant  $\alpha$  become available from Rb measurement.
- These lead to:
  - The theoretical value of electron  $g-2$  is obtained by the uncertainty of  $0.77 \times 10^{-12}$ , and it is in good agreement with the experimental value measured up to the uncertainty of  $0.28 \times 10^{-12}$ .
  - From the measurement and the theory of electron  $g-2$ , the most precise value of the fine structure constant  $\alpha$  is obtained, whose uncertainty is  $0.25 \times 10^{-9}$ .
  - For the muon  $g-2$ , the QED contribution has been pinned down precisely enough for the current and near-future experiments.
- These 10th-order contributions are obtained by numerical means, in which the automation in generating the numerical integration code speeds up drastically for those complicated Feynman diagrams.